Published in final edited form as:

Abdom Radiol (NY). 2020 November ; 45(11): 3545–3556. doi:10.1007/s00261-020-02677-2.

Collagen-targeted Molecular Imaging in Diffuse Liver Diseases

Iris Y. Zhou[1,2,3], **Kenneth K. Tanabe**[4], **Bryan C. Fuchs**[5], **Peter Caravan**[1,2,3]

[1]Athinoula A. Martinos Center for Biomedical Imaging, Charlestown, MA, USA

[2]Harvard Medical School, Boston, MA, USA

[3]Institute for Innovation in Imaging (i3), Department of Radiology, Massachusetts General Hospital, Charlestown, MA, USA

[4]Division of Surgical Oncology, Massachusetts General Hospital and Harvard Medical School, Boston, MA, USA

[5]Ferring Research Institute, San Diego, CA, USA

Abstract

Liver fibrosis is a common pathway shared by all progressive chronic liver disease (CLD) regardless of the underlying etiologies. With liver biopsy being the gold standard in assessing fibrosis degree, there is a large unmet clinical need to develop noninvasive imaging tools that can directly and repeatedly quantify fibrosis throughout the liver for a more accurate assessment of disease burden, progression, and treatment response. Type I collagen is a particularly attractive target for molecular imaging as its excessive deposition is specific to fibrosis, and it is present in concentrations suitable for many imaging modalities. Novel molecular MRI contrast agents designed to bind with collagen provide direct quantification of collagen deposition, which have been validated across animal species and liver injury models. Collagen targeted molecular imaging probes hold great promise not only as a tool for initial staging and surveillance of fibrosis progression, but also as a marker of fibrosis regression in drug trials.

Keywords

molecular imaging; collagen; ECM; fibrosis; MRI

Chronic liver disease (CLD) is a common and serious public health burden. The major causes of CLD include nonalcoholic fatty liver disease (NAFLD)/nonalcoholic steatohepatitis (NASH), hepatic viral infections, alcohol abuse, chronic alteration of metabolism, or persistent autoimmune reaction [1]. NAFLD and NASH are the leading forms of CLD, and their worldwide prevalence continues to grow due to increasing incidence of diabetes and obesity in the USA and other regions [2,3]. Liver fibrosis is a

Corresponding Author: Peter Caravan, Ph.D., 149 13th St, Boston, MA 02129, USA, Phone: 617-643-0193, caravan@nmr.mgh.harvard.edu.

Conflict of interest: P.C. has equity in and is a consultant to Collagen Medical LLC which owns the patent rights to EP-3533 and CM-101, has equity in Reveal Pharmaceuticals Inc, and has research support from Pliant Therapeutics, Celgene, and Indalo Therapeutics. B.C.F. is an employee of Ferring Pharmaceuticals.

hallmark shared by almost all causes of progressive CLD. Without removal of exposure to the specific etiology, fibrosis tends to progress, leading to hepatic dysfunction, portal hypertension, and ultimately culminating in liver cirrhosis. Moreover, the presence and severity of fibrosis are the main prognostic factors for clinical outcomes in patients with CLD. Therefore, it is crucial to be able to differentiate liver fibrosis stages since treatment decision and monitoring algorithms are related to the degree of fibrosis [4–6].

Liver biopsy is still considered the gold standard for detecting and staging liver fibrosis, however, biopsy is invasive with risk of complications such as bleeding, can be limited due to sampling error from the heterogenous distribution of pathology, and demonstrates inter-observer variation on pathology interpretation [7,8]. Serum markers of liver disease are potential non-invasive alternative to liver biopsy as they are easily obtained, are less affected by sampling error, and can be repeated serially. However, most of these markers lack sensitivity and/or specificity, may detect false negative in end-stage CLD, and can be confounded by a wide variety of extrahepatic disorders [9,10]. Ultrasound and MR-based elastography are two widely used modalities for clinical detection and staging of liver fibrosis by measuring tissue stiffness [11–13]. Both methods reliably distinguish patients with moderate/advanced fibrosis from those with lesser degrees or no fibrosis [14], however, their diagnostic performance is limited in distinction between adjacent stages of fibrosis [15]. Other limitations include the technical difficulties of performing ultrasound elastography in patients with ascites/morbid obesity [16–18] or failures of performing MR elastography in patients with high iron overload due to low signal-to-noise ratio [19–21]. Thus, development of a noninvasive, accurate, and reproducible test to quantify liver fibrosis would be of great importance for early diagnosis, serial monitoring of disease progression in CLD, and therapy response assessment.

Repetitive or persistent hepatic injury triggers a cascade of wound healing responses, leading to a progressive substitution of liver parenchyma by scar tissue, or fibrosis. A characteristic feature of the fibrotic microenvironment associated with CLD is excessive deposition of extracellular matrix (ECM) proteins [22]. Type I collagen is the most abundant ECM protein in mammals and the main component of fibrotic tissue [23]. In cirrhotic liver, collagen was upregulated four- to seven-fold with type I collagen being the predominant type [24]. Therefore, type I collagen has been pursued as a molecular target for a direct assessment of liver fibrosis. Our group has led the efforts to develop biochemically targeted imaging contrast agents to adhere with high affinity to type I collagen for the detection and staging of liver fibrosis and to monitor treatment response.

Detecting and staging fibrosis

EP-3533 is a molecular probe that contains a 16-amino acid disulfide-bridged cyclic peptide that provides specific affinity to type I collagen and three Gd-DTPA moieties to boost MRI signal enhancement [25,26]. The feasibility of EP-3533–enhanced MRI for detection of liver fibrosis was first evaluated using rat and mouse models [27]. Liver fibrosis was induced in rats with diethylnitrosamine (DEN) and in mice with carbon tetrachloride (CCl_4) and confirmed histologically. Animals were imaged prior to and immediately following i.v. administration of either collagen-targeted probe EP-3533 or non-targeted control probe Gd-

DTPA for 60 min post-injection. Significantly slower signal washout and delayed peak enhancements in EP-3533-enhanced MRI of the injured livers indicates that EP-3533 was retained longer in fibrotic tissue than in the livers of healthy control animals (Figure 1). Gd-DTPA-enhanced MR could not distinguish fibrotic from control animals. The EP-3533 gadolinium concentration in the liver showed strong positive correlations with total collagen determined biochemically by hydroxyproline analysis and also with histopathological scoring of fibrosis using the Ishak system. In this initial study, we demonstrated that MRI with a type I collagen-targeted probe can distinguish liver fibrosis in two animal models of disease. However, the study was not powered to address the question of whether EP-3533 enhanced MRI could stage fibrosis because the animals were only imaged at a single time point during disease progression.

To study the staging ability of EP-3533-enhanced MRI as compared to other MRI techniques, we followed with a second study in CCl_4-injured mice where the duration of chemical toxin administration was varied [28]. We found greater enhancement post-EP-3533 in the liver of the fibrotic animal than the controls (Figure 2A). The readouts from EP-3533-enhanced MRI were compared with T1, T2, and T1rho relaxation times, apparent diffusion coefficient (ADC), and magnetization transfer ratio (MTR) measurements obtained prior to contrast agent injection. The most sensitive MRI biomarker was the change in liver-to-muscle contrast to noise ratio (ΔCNR) after EP-3533 injection (Figure 2B). We observed a strong positive linear correlation between ΔCNR and liver hydroxyproline levels as well as ΔCNR and histopathological Ishak fibrosis scoring (Figure 2C–D). In addition, the area under the receiver operating curve (AUROC) for distinguishing early (Ishak ≤ 3) from advanced (Ishak ≥ 4) fibrosis was 0.94. Despite literature reports of relaxation times (T1, T2 or T1rho), ADC and MTR as sensitive markers of liver fibrosis, we only observed weak correlations of these parameters with liver hydroxyproline levels in this animal model. Only T1rho measurement could distinguish fibrotic from healthy livers, but it could not differentiate moderate (Ishak 2–3) from severe (Ishak 4–5) fibrosis. In contrast, the other MR measurements (T1, T2, ADC, MTR) could not classify animals into groups based on Ishak scoring.

These first two studies were performed on a high field (4.7T) dedicated animal scanner and disease was quantified in a few axial slices using 2D imaging methods. We next extended the utility of this work by imaging on a standard 1.5T clinical MRI scanner and using a three-dimensional (3D) imaging method that could quantify fibrosis over the entire liver. The ability of MRI to stage severity of fibrosis with EP-3533 was further tested in a rat model of biliary stasis using bile duct ligation (BDL) [29]. Fibrosis quantification was further enhanced by using a respiratory-gated 3D inversion recovery imaging sequence that allows us to measure the change in longitudinal relaxation rate (ΔR1) induced by EP-3533 on a pixel-wise basis throughout the entire liver. Since ΔR1 is linearly proportional to gadolinium concentration, it has the potential to provide a more quantitative and robust metric than ΔCNR for the assessment of fibrosis, and to measure disease heterogeneity within the liver. ΔR1 increased significantly and progressively as a function of time after BDL compared to control rats who underwent a sham procedure. The MRI quantitative readout correlated closely with ex vivo quantification of fibrosis measured by the collagen proportional area (CPA) of Sirius Red stained sections and hydroxyproline content. Receiver

operating characteristic curve analysis demonstrated that ΔR1 detects fibrosis (CPA ≤ 3% vs. CPA > 3%) with an AUROC of 0.84, distinguishes early fibrosis from significant fibrosis (CPA ≤ 6% vs. CPA > 6%) with an AUROC of 0.94, and distinguishes significant fibrosis from severe fibrosis (CPA ≤ 9% vs. CPA >9%) with an AUROC of 0.94, p <0.0001.

Evaluating treatment responses

There are a large number of drug candidates targeting different signaling pathways under evaluation in preclinical and clinical trials [30–32], but a major obstacle has been the slow rate of progression or regression of CLD in humans, coupled with a lack of sensitive and non-invasive means to assess fibrosis or active fibrogenesis [33]. Together, these factors create an enormous cost risk for anti-fibrotic drug development, since clinical trials require large patient populations treated for long periods of time to reach a clinically significant endpoint. Thus, a biomarker of liver fibrosis that could accurately assess fibrogenesis early in treatment would not only be extraordinarily useful in enabling the evaluation of much larger pools of candidate therapies in clinical trials, but also might provide the early evidence of efficacy needed to incentivize investigators and pharmaceutical sponsors to support long-term trials.

Historically, assessment of treatment response has relied on histologic analysis [34,35]. Elastography-based liver stiffness measurements have been explored for monitoring regression of fibrosis in patients with chronic viral hepatitis after antiviral treatment [36–39] and detecting treatment associated risk of liver fibrosis [40]. However, the evaluation of liver fibrosis with stiffness measurement can be confounded by many coexistent conditions including necroinflammation, edema, venous congestion, biliary obstruction, and any diffuse infiltrative disease such as amyloidosis [41,42]. Having shown the feasibility of EP-3533 in detecting and staging liver fibrosis, we further investigated its ability in assessing treatment response. We first used a common approach of toxin withdrawal as a model of fibrosis regression. Mice injured with CCl_4 for 18 weeks were compared to mice injured with CCl_4 for 9 weeks followed by 9 weeks of withdrawal. Withdrawal of CCl_4 improved liver disease as assessed by Sirius Red staining with the Ishak score improving by 2 stages on average. However, MRI with EP-3533 could not detect a difference in fibrosis stage between these two groups of mice. It has been reported that even with histological improvement after CCl_4 withdrawal, total collagen as assessed by hydroxyproline analysis did not decrease for at least 12 weeks [43]. Consistently, we found the hydroxyproline levels did not differ significantly between the animals that had CCl_4 withdrawal and those that continued to receive CCl_4. These results therefore further highlight the specificity of EP-3533 to collagen.

To further determine the ability of collagen imaging with EP-3533 to detect treatment response, we measured fibrosis content in rapamycin treated BDL rats [29]. While there are no FDA-approved drugs for treating liver fibrosis, previous studies have shown that rapamycin is effective in reducing fibrosis in the rat BDL model but with significant variability in response [44]. Four days after bile duct ligation, rats were treated daily with rapamycin and imaged on day 18. Rapamycin treatment resulted in a significant reduction in ΔR1 compared to vehicle treated animals and this was supported by significantly lower levels of hydroxyproline and CPA in the rapamycin treated rats compared to vehicle treated

controls. However, the range of reduction in hydroxyproline and CPA was broad indicating that some animals responded well to rapamycin treatment while others did not. Using the receiver operating characteristic (ROC) analysis described above, cutoff values for ΔR1 could be assigned to prospectively and objectively distinguish animals with severe disease (non-responders) from those who responded well to treatment (Figure 3A). Using this criterion, we found that the ΔR1 value correctly predicted rapamycin response in 11 out of 12 rats compared to the CPA truth standard. In addition, 3D molecular MRI enabled characterization of intrahepatic heterogeneity throughout the whole liver in a rapamycin non-responder rat (Figure 3B). Molecular MRI showed severe fibrosis in the right lobe but mild-to-moderate fibrosis in the left lobe of the liver which was subsequently confirmed by histology (Figure 3C–D).

In another study, EP-3533 enhanced MRI was used to noninvasively monitor the treatment effect of a novel farnesoid X receptor agonist, EDP-305, in the rat BDL model [45]. BDL rats were treated with either low or high doses of EDP-305 starting on day 4 after BDL and were imaged on day 18. A significant reduction in liver ΔR1 was found in BDL rats receiving high-dose EDP-305 treatment than BDL control, consistent with the CPA, hydroxyproline analysis, and fibrogenic gene expression findings of marked reduction of hepatic fibrosis in response to EDP-305.

Improved collagen imaging MR probes

EP-3533 utilizes the linear chelate Gd-DTPA as the signal generating moiety. However these linear chelates are associated with a higher incidence of nephrogenic systemic fibrosis (NSF) and appear to also result in greater retention of Gd [46]. On the other hand, macrocyclic chelators like Gd-DOTA have a much lower incidence of NSF and appear to give lower amounts of Gd retention [46,47]. To improve the clinical translational potential of EP-3533, we developed a new version, CM-101, which has the linear Gd-DTPA chelate replaced by the highly stable macrocyclic Gd-DOTA chelate [48]. Pharmacokinetic analysis demonstrated that CM-101 exhibited faster rapid blood clearance than EP-3533 which results in the ability to shorten the time period between injection and delayed liver imaging. At two independent imaging labs, CM-101 detected fibrosis in mouse CCl_4 and rat BDL models of liver fibrosis (Figure 4). Biodistribution analysis demonstrated that incorporation of the macrocyclic Gd-DOTA chelate resulted in minimal accumulation of gadolinium in bone or other tissue compared to EP-3533.

In a recent study by another group led by Yang, the same type I collagen targeting peptide used in EP-3533 and CM-101 was used in a protein-based contrast agent (ProCA32.collagen1). ProCA32 is a small protein that was engineered to bind tightly to gadolinium and to have a very high relaxivity. Grafting the collagen specific peptide to ProCA32 created ProCA32.collagen1 and this reagent was used for the early diagnosis and noninvasive detection of liver fibrosis in alcohol/chemical-induced mouse models of liver fibrosis and a diet-induced mouse model of NASH [49]. ProCA32.collagen1 was demonstrated to detect early-stage alcohol-induced liver fibrosis (Ishak stage 3 of 6) and early-stage NASH (Mild-1A, zone 3, perisinusoidal or Ishak stage 1 of 6) using both longitudinal and transverse relaxation (R1 and R2) maps at 24 h post-injection. ΔR1

quantification of ProCA32.collagen1 can distinguish early-stage (Ishak stage 3) from late-stage fibrosis (Ishak stage 5), which correlated with histologic quantification of fibrosis. Because of its much larger size, ProCA32.collagen1 has a longer blood residency time than either EP-3533 or CM-101, and so the delayed imaging took place hours after injection or the next day compared to within 10 – 40 minutes with EP-3533 or CM-101.

Targeting oxidized collagen as a marker of active fibrogenesis

Fibrogenesis, or the active deposition of ECM, is characterized by high levels of allysine, a reactive aldehyde generated as part of a lysyl oxidase (LOX)-mediated collagen cross-linking process. In fibrogenesis, LOX oxidation of collagen results in the buildup of an allysine rich oxidized collagen epitope. These allysine residues undergo cross-linking reactions with other collagen monomers resulting in a stable matrix. During active disease, the pool of oxidized collagen is constantly replenished but in chronic, stable scar tissue the oxidized collagen has all been consumed into crosslinks. Allysine aldehyde-targeting imaging probes that measure oxidized collagen thus can be used to monitor fibrogenesis [50,51]. The hydrazide containing, aldehyde targeting agent Gd-Hyd detected and staged disease progression caused by CCl_4 injury in mice and reported on reduced fibrogenesis in mice after withdrawal of CCl_4 (Figure 5) [52]. The imaging data mirrored disease progression and resolution as assessed by histology and lysyl oxidase gene expression. In mice fed with a choline-deficient, L-amino acid-defined, high-fat diet (CDAHFD) as a model of nonalcoholic steatohepatitis (NASH), Gd-Hyd detected reduced fibrogenesis after treatment with the farnesoid X receptor agonist EDP-305, corroborated by multiple methodologies, including picrosirius red collagen staining, hydroxyproline biochemical quantification, and lysyl oxidase gene expression analyses [45]. These data suggest that Gd-Hyd could be used to monitor disease progression and regression.

Multiparametric capability of MRI

In addition to molecular MRI in liver, state-of-the-art MRI techniques in current practice and in development for noninvasive assessment of CLD include MR elastography, diffusion-weighted imaging, MRI quantification of liver fat or iron content and functional MRI using hepatobiliary contrast agents that are taken up specifically by hepatocytes. Molecular imaging can be readily performed in conjunction with these advanced MRI techniques to provide a more comprehensive assessment of CLD. For instance, Gd-Hyd–enhanced MRI of oxidized collagen and Dixon MRI-based quantitative fat imaging were used in a mouse model for multi-parametric MRI assessment of NASH [45]. In a DEN-induced rat model of fibrosis, collagen imaging with EP-3533 was shown to be most sensitive to early fibrosis, while tissue stiffness assessed by MR elastography was more sensitive to advanced fibrosis [53]. Combining these two measurements in a single exam to give a composite score resulted in increased diagnostic accuracy for all stages of fibrosis [53].

Recently, EP-3533 imaging of collagen in the presence and absence of inflammation was investigated in DEN-injured rats where hepatic inflammation was assessed by a fibrin-targeted EP-2104R MRI probe [54]. Tissue injury triggers extravascular coagulation that leads to fibrin deposition in the ECM [55]. EP-2104R is a fibrin-specific molecular probe

that has been used for molecular imaging of extravascular fibrin in mouse models of cancer and pulmonary fibrosis [56,57]. Collagen imaging with EP-3533 showed equivalent T1 change when imaging rats 1 day or 7 days post-DEN, consistent with equivalent fibrosis assessed by Ishak score. Signal enhancement with EP-2104R was significantly higher in animals imaged at 1 day post-DEN compared with 7 days post-DEN or control rats, consistent with a significantly higher histological activity index score for inflammation in the livers of animals imaged within one day of their last DEN administration. The specificity of the targeted probes for either inflammation of fibrosis allows us to determine the status of each feature, which have important diagnostic and prognostic implications of CLD.

In a most recent multi-parametric MRI study, advanced MRI methods including molecular MRI with the type-1-collagen-specific probe EP-3533 and the allysine-targeted fibrogenesis probe Gd-Hyd, MR elastography, and native T1, were used to characterize fibrosis and to assess treatment response in rats fed with CDAHFD as a model of NASH [58]. Liver ΔR1 is higher following EP-3533 administration to the CDAHFD rats as compared to the control or treated animals, indicative of greater probe uptake as a result of collagen binding (Figure 6A). Similar to EP-3533, larger ΔR1 changes after the injection of fibrogenesis probe Gd-Hyd were seen in animals receiving CDAHFD (Figure 6B). Using MR elastography, we observed much larger changes in tissue stiffness in the CDAHFD rats showing advanced fibrosis, but MRE could not distinguish rats with early onset of fibrosis from those with no fibrosis. While liver fibrosis is consistently associated with increased hepatic parenchymal stiffness, the opposite is not always true. Acute inflammation, severe steatosis, or increased postprandial portal blood flow have been found to independently elevate hepatic stiffness [59,12,60]. Among the imaging methods investigated, the collagen-targeted molecular MRI probe most accurately detected early onset of liver fibrosis with an area under the receiver operating characteristic curve (AUC) of 0.95, followed by native T1, Gd-Hyd and MR elastography with AUCs of 0.90, 0.84, 0.65, respectively. Native T1 measurement with iron content correction was used to stage liver fibrosis [61,62] and we found a relatively large AUC for native T1 to detect early stage fibrosis in the CDAHFD rats. However, upon closer analysis this T1 change appeared to be driven by increased steatosis rather than fibrosis, as shown by a strong correlation between the native T1 measurement and fat fraction measured by histology or by Dixon MRI. The fibrogenesis imaging probe Gd-Hyd can stage fibrosis and had the highest accuracy (92%) in detecting responder and non-responders in treatment of NASH, compared to MR elastography (88%), EP-3533 (77%), and native T1 (54%). The advanced MRI techniques applied there are complementary in their capture of the fibrotic process. All techniques were performed in a single protocol, highlighting the strength of MRI for characterizing liver disease in the context of NASH. The rich information provided by such imaging protocol raises new possibilities for clinical imaging and for assessing treatment response for new therapies in development.

Challenges and Outlook

Liver fibrosis is a common result of progressive chronic liver disease regardless of the underlying etiologies. Here we describe different molecular MR approaches to detecting and staging fibrosis. Although fibrosis is common to CLD, other aspects of pathology, e.g. presence of inflammation, steatosis, necrosis, ascites, different metabolic derangements, are

unique to the individual liver diseases. It is important to bear in mind that no animal model completely replicates all aspects of human disease. That being said, the transdifferentiation of stellate cells into myofibroblasts is thought to be fairly similar across all CLD. In other words, type I collagen and lysyl oxidase modified collagen are generic for liver fibrosis regardless of disease etiology. However the etiology itself could impact the imaging, e.g. does fat associated with NAFLD/NASH interfere with probe binding? So far, it appears that these molecular probes are very specific to liver fibrosis. By using different animal models (toxin, diet, biliary stasis) with different extents of liver injury, it has been possible to demonstrate the ability to quantify fibrosis in the absence and presence of steatosis, inflammation, and hepatocellular carcinoma. Similarly, it was repeatedly shown that molecular MRI could detect and monitor response to treatment whether this was dietary or pharmacological. Ultimately this same type of validation will be required in human clinical trials.

Among the emerging fibrosis imaging methods, elastography-based techniques are the most widely used. Despite evidence showing their utility as diagnostic and prognostic tools, confounding factors such as obesity, inflammation, and iron overload have been noted. Direct targeting of the fibrotic components using molecular MRI offers an innovative approach with potential high specificity, and is complementary to elastography. Molecular MRI can be performed in conjunction with other types of high-resolution imaging that can provide details on liver anatomy and function. However, several challenges exist in developing and translating molecular MRI probes, which are regulated as drugs. Like most drugs, extensive safety evaluations in rodents and non-rodents are required and manufacturing processes and controls must be established before first-in-human evaluation. The manufacturing and nonclinical safety studies represent a major economic barrier to translation. For regulatory approval, the molecular probe must show demonstrated efficacy (sensitivity and specificity) to detect and/or stage fibrosis in prospective clinical trials. Ultimately outcome data will be required to establish the clinical utility of the molecular probes in order to drive reimbursement. However with the likely approvals of new, expensive anti-inflammatory/anti-viral/antifibrotic therapeutics, there will be a need to identify patients who would best benefit from these treatments and/or to monitor whether the treatment is likely to be effective. Molecular MRI is uniquely poised to fulfill this need.

Conclusion

The studies described here serve to validate collagen-specific molecular MRI as a means to accurately stage liver fibrosis across animal species (rat and mouse) and liver injury models (CCl_4, DEN, BDL, and CDAHFD). EP-3533 and its derivatives have also been used to detect and stage disease in models of cardiac [26,25,63], pulmonary [64], and muscle fibrosis [65], as well as in cancer models with a strong desmoplastic reaction [66] which further support collagen molecular MR as a tool to noninvasively assess fibrosis. Positron emission tomography probes utilizing the same collagen-binding peptide or targeting allysine have also been reported [67–69], and the use of the collagen-targeted PET probe to image pulmonary fibrosis in patients with idiopathic pulmonary fibrosis has been reported which further supports the clinical translational potential of this technology [70].

Advances in molecular imaging, particularly with the development of molecularly targeted probes, have the potential to revolutionize how we evaluate various liver pathologic conditions. The ability to quantify liver fibrosis stages noninvasively is highly desired as it allows noninvasive assessment of disease burden, progression, and treatment response. The molecular imaging probes described here represent the first steps towards these goals. While the work was performed in preclinical models, the next steps will hinge upon improved and standardized imaging protocols and post-processing methods and further optimization of the molecular probes, for successful translation into clinical application.

Funding:

We acknowledge support from the National Institute of Diabetes and Digestive and Kidney Diseases with grants DK104956, DK104302, DK121789.

References

1. Friedman SL (2008) Mechanisms of hepatic fibrogenesis. Gastroenterology 134 (6):1655–1669. doi:10.1053/j.gastro.2008.03.003 [PubMed: 18471545]
2. Vernon G, Baranova A, Younossi ZM (2011) Systematic review: the epidemiology and natural history of non-alcoholic fatty liver disease and non-alcoholic steatohepatitis in adults. Aliment Pharmacol Ther 34 (3):274–285. doi:10.1111/j.1365-2036.2011.04724.x [PubMed: 21623852]
3. Estes C, Anstee QM, Arias-Loste MT, Bantel H, Bellentani S, Caballeria J, Colombo M, Craxi A, Crespo J, Day CP, Eguchi Y, Geier A, Kondili LA, Kroy DC, Lazarus JV, Loomba R, Manns MP, Marchesini G, Nakajima A, Negro F, Petta S, Ratziu V, Romero-Gomez M, Sanyal A, Schattenberg JM, Tacke F, Tanaka J, Trautwein C, Wei L, Zeuzem S, Razavi H (2018) Modeling NAFLD disease burden in China, France, Germany, Italy, Japan, Spain, United Kingdom, and United States for the period 2016–2030. J Hepatol 69 (4):896–904. doi:10.1016/j.jhep.2018.05.036 [PubMed: 29886156]
4. Bruix J, Sherman M, Practice Guidelines Committee AAftSoLD (2005) Management of hepatocellular carcinoma. Hepatology 42 (5):1208–1236. doi:10.1002/hep.20933 [PubMed: 16250051]
5. Friedman SL (2003) Liver fibrosis -- from bench to bedside. J Hepatol 38 Suppl 1:S38–53. doi:10.1016/s0168-8278(02)00429-4 [PubMed: 12591185]
6. Puoti C, Guarisco R, Bellis L, Spilabotti L (2009) Diagnosis, management, and treatment of hepatitis C. Hepatology 50 (1):322; author reply 324–325. doi:10.1002/hep.23015 [PubMed: 19472312]
7. Sumida Y, Nakajima A, Itoh Y (2014) Limitations of liver biopsy and non-invasive diagnostic tests for the diagnosis of nonalcoholic fatty liver disease/nonalcoholic steatohepatitis. World journal of gastroenterology 20 (2):475–485. doi:10.3748/wjg.v20.i2.475 [PubMed: 24574716]
8. Bravo AA, Sheth SG, Chopra S (2001) Liver biopsy. N Engl J Med 344 (7):495–500. doi:10.1056/NEJM200102153440706 [PubMed: 11172192]
9. Rosenberg WM, Voelker M, Thiel R, Becka M, Burt A, Schuppan D, Hubscher S, Roskams T, Pinzani M, Arthur MJ, European Liver Fibrosis G (2004) Serum markers detect the presence of liver fibrosis: a cohort study. Gastroenterology 127 (6):1704–1713. doi:10.1053/j.gastro.2004.08.052 [PubMed: 15578508]
10. Parkes J, Guha IN, Roderick P, Rosenberg W (2006) Performance of serum marker panels for liver fibrosis in chronic hepatitis C. J Hepatol 44 (3):462–474. doi:10.1016/j.jhep.2005.10.019 [PubMed: 16427156]
11. Chen J, Talwalkar JA, Yin M, Glaser KJ, Sanderson SO, Ehman RL (2011) Early detection of nonalcoholic steatohepatitis in patients with nonalcoholic fatty liver disease by using MR elastography. Radiology 259 (3):749–756. doi:10.1148/radiol.11101942 [PubMed: 21460032]
12. Salameh N, Larrat B, Abarca-Quinones J, Pallu S, Dorvillius M, Leclercq I, Fink M, Sinkus R, Van Beers BE (2009) Early detection of steatohepatitis in fatty rat liver by using MR elastography. Radiology 253 (1):90–97. doi:10.1148/radiol.2523081817 [PubMed: 19587308]

13. Nobili V, Vizzutti F, Arena U, Abraldes JG, Marra F, Pietrobattista A, Fruhwirth R, Marcellini M, Pinzani M (2008) Accuracy and reproducibility of transient elastography for the diagnosis of fibrosis in pediatric nonalcoholic steatohepatitis. Hepatology 48 (2):442–448. doi:10.1002/hep.22376 [PubMed: 18563842]

14. Yin M, Glaser KJ, Talwalkar JA, Chen J, Manduca A, Ehman RL (2016) Hepatic MR Elastography: Clinical Performance in a Series of 1377 Consecutive Examinations. Radiology 278 (1):114–124. doi:10.1148/radiol.2015142141 [PubMed: 26162026]

15. Hagan M, Asrani SK, Talwalkar J (2015) Non-invasive assessment of liver fibrosis and prognosis. Expert Rev Gastroenterol Hepatol 9 (10):1251–1260. doi:10.1586/17474124.2015.1075391 [PubMed: 26377444]

16. Sandrin L, Fourquet B, Hasquenoph JM, Yon S, Fournier C, Mal F, Christidis C, Ziol M, Poulet B, Kazemi F, Beaugrand M, Palau R (2003) Transient elastography: a new noninvasive method for assessment of hepatic fibrosis. Ultrasound in medicine & biology 29 (12):1705–1713 [PubMed: 14698338]

17. Ziol M, Handra-Luca A, Kettaneh A, Christidis C, Mal F, Kazemi F, de Ledinghen V, Marcellin P, Dhumeaux D, Trinchet JC, Beaugrand M (2005) Noninvasive assessment of liver fibrosis by measurement of stiffness in patients with chronic hepatitis C. Hepatology 41 (1):48–54. doi:10.1002/hep.20506 [PubMed: 15690481]

18. Cohen EB, Afdhal NH (2010) Ultrasound-based hepatic elastography: origins, limitations, and applications. J Clin Gastroenterol 44 (9):637–645. doi:10.1097/MCG.0b013e3181e12c39 [PubMed: 20844365]

19. Singh S, Venkatesh SK, Wang Z, Miller FH, Motosugi U, Low RN, Hassanein T, Asbach P, Godfrey EM, Yin M, Chen J, Keaveny AP, Bridges M, Bohte A, Murad MH, Lomas DJ, Talwalkar JA, Ehman RL (2015) Diagnostic performance of magnetic resonance elastography in staging liver fibrosis: a systematic review and meta-analysis of individual participant data. Clin Gastroenterol Hepatol 13 (3):440–451 e446. doi:10.1016/j.cgh.2014.09.046 [PubMed: 25305349]

20. Huwart L, Sempoux C, Vicaut E, Salameh N, Annet L, Danse E, Peeters F, ter Beek LC, Rahier J, Sinkus R, Horsmans Y, Van Beers BE (2008) Magnetic resonance elastography for the noninvasive staging of liver fibrosis. Gastroenterology 135 (1):32–40. doi:10.1053/j.gastro.2008.03.076 [PubMed: 18471441]

21. Horowitz JM, Venkatesh SK, Ehman RL, Jhaveri K, Kamath P, Ohliger MA, Samir AE, Silva AC, Taouli B, Torbenson MS, Wells ML, Yeh B, Miller FH (2017) Evaluation of hepatic fibrosis: a review from the society of abdominal radiology disease focus panel. Abdom Radiol (NY) 42 (8):2037–2053. doi:10.1007/s00261-017-1211-7 [PubMed: 28624924]

22. Hernandez-Gea V, Friedman SL (2011) Pathogenesis of liver fibrosis. Annu Rev Pathol 6:425–456. doi:10.1146/annurev-pathol-011110-130246 [PubMed: 21073339]

23. Exposito JY, Valcourt U, Cluzel C, Lethias C (2010) The fibrillar collagen family. Int J Mol Sci 11 (2):407–426. doi:10.3390/ijms11020407 [PubMed: 20386646]

24. Rojkind M, Giambrone MA, Biempica L (1979) Collagen types in normal and cirrhotic liver. Gastroenterology 76 (4):710–719 [PubMed: 421999]

25. Helm PA, Caravan P, French BA, Jacques V, Shen L, Xu Y, Beyers RJ, Roy RJ, Kramer CM, Epstein FH (2008) Postinfarction myocardial scarring in mice: molecular MR imaging with use of a collagen-targeting contrast agent. Radiology 247 (3):788–796. doi:10.1148/radiol.2473070975 [PubMed: 18403626]

26. Caravan P, Das B, Dumas S, Epstein FH, Helm PA, Jacques V, Koerner S, Kolodziej A, Shen L, Sun WC, Zhang Z (2007) Collagen-targeted MRI contrast agent for molecular imaging of fibrosis. Angew Chem Int Ed Engl 46 (43):8171–8173. doi:10.1002/anie.200700700 [PubMed: 17893943]

27. Polasek M, Fuchs BC, Uppal R, Schuhle DT, Alford JK, Loving GS, Yamada S, Wei L, Lauwers GY, Guimaraes AR, Tanabe KK, Caravan P (2012) Molecular MR imaging of liver fibrosis: a feasibility study using rat and mouse models. J Hepatol 57 (3):549–555. doi:10.1016/j.jhep.2012.04.035 [PubMed: 22634342]

28. Fuchs BC, Wang H, Yang Y, Wei L, Polasek M, Schuhle DT, Lauwers GY, Parkar A, Sinskey AJ, Tanabe KK, Caravan P (2013) Molecular MRI of collagen to diagnose and stage liver fibrosis. J Hepatol 59 (5):992–998. doi:10.1016/j.jhep.2013.06.026 [PubMed: 23838178]

29. Farrar CT, DePeralta DK, Day H, Rietz TA, Wei L, Lauwers GY, Keil B, Subramaniam A, Sinskey AJ, Tanabe KK, Fuchs BC, Caravan P (2015) 3D molecular MR imaging of liver fibrosis and response to rapamycin therapy in a bile duct ligation rat model. J Hepatol 63 (3):689–696. doi:10.1016/j.jhep.2015.04.029 [PubMed: 26022693]
30. Inagaki Y, Higashiyama R, Higashi K (2012) Novel anti-fibrotic modalities for liver fibrosis: molecular targeting and regenerative medicine in fibrosis therapy. J Gastroenterol Hepatol 27 Suppl 2:85–88. doi:10.1111/j.1440-1746.2011.07006.x [PubMed: 22320923]
31. Kisseleva T, Brenner DA (2011) Anti-fibrogenic strategies and the regression of fibrosis. Best Pract Res Clin Gastroenterol 25 (2):305–317. doi:10.1016/j.bpg.2011.02.011 [PubMed: 21497747]
32. Friedman SL, Sheppard D, Duffield JS, Violette S (2013) Therapy for fibrotic diseases: nearing the starting line. Sci Transl Med 5 (167):167sr161. doi:10.1126/scitranslmed.3004700
33. Popov Y, Schuppan D (2009) Targeting liver fibrosis: strategies for development and validation of antifibrotic therapies. Hepatology 50 (4):1294–1306. doi:10.1002/hep.23123 [PubMed: 19711424]
34. Neuschwander-Tetri BA, Loomba R, Sanyal AJ, Lavine JE, Van Natta ML, Abdelmalek MF, Chalasani N, Dasarathy S, Diehl AM, Hameed B, Kowdley KV, McCullough A, Terrault N, Clark JM, Tonascia J, Brunt EM, Kleiner DE, Doo E, Network NCR (2015) Farnesoid X nuclear receptor ligand obeticholic acid for non-cirrhotic, non-alcoholic steatohepatitis (FLINT): a multicentre, randomised, placebo-controlled trial. Lancet 385 (9972):956–965. doi:10.1016/S0140-6736(14)61933-4 [PubMed: 25468160]
35. Sanyal AJ, Brunt EM, Kleiner DE, Kowdley KV, Chalasani N, Lavine JE, Ratziu V, McCullough A (2011) Endpoints and clinical trial design for nonalcoholic steatohepatitis. Hepatology 54 (1):344–353. doi:10.1002/hep.24376 [PubMed: 21520200]
36. Vergniol J, Foucher J, Terrebonne E, Bernard PH, le Bail B, Merrouche W, Couzigou P, de Ledinghen V (2011) Noninvasive tests for fibrosis and liver stiffness predict 5-year outcomes of patients with chronic hepatitis C. Gastroenterology 140 (7):1970–1979, 1979 e1971–1973. doi:10.1053/j.gastro.2011.02.058 [PubMed: 21376047]
37. Kim JH, Kim MN, Han KH, Kim SU (2015) Clinical application of transient elastography in patients with chronic viral hepatitis receiving antiviral treatment. Liver international : official journal of the International Association for the Study of the Liver 35 (4):1103–1115. doi:10.1111/liv.12628 [PubMed: 24976523]
38. Suda T, Okawa O, Masaoka R, Gyotoku Y, Tokutomi N, Katayama Y, Tamano M (2017) Shear wave elastography in hepatitis C patients before and after antiviral therapy. World J Hepatol 9 (1):64–68. doi:10.4254/wjh.v9.i1.64 [PubMed: 28105260]
39. Bachofner JA, Valli PV, Kroger A, Bergamin I, Kunzler P, Baserga A, Braun D, Seifert B, Moncsek A, Fehr J, Semela D, Magenta L, Mullhaupt B, Terziroli Beretta-Piccoli B, Mertens JC (2017) Direct antiviral agent treatment of chronic hepatitis C results in rapid regression of transient elastography and fibrosis markers fibrosis-4 score and aspartate aminotransferase-platelet ratio index. Liver international : official journal of the International Association for the Study of the Liver 37 (3):369–376. doi:10.1111/liv.13256 [PubMed: 27678216]
40. Laharie D, Seneschal J, Schaeverbeke T, Doutre MS, Longy-Boursier M, Pellegrin JL, Chabrun E, Villars S, Zerbib F, de Ledinghen V (2010) Assessment of liver fibrosis with transient elastography and FibroTest in patients treated with methotrexate for chronic inflammatory diseases: a case-control study. J Hepatol 53 (6):1035–1040. doi:10.1016/j.jhep.2010.04.043 [PubMed: 20801541]
41. Hoodeshenas S, Yin M, Venkatesh SK (2018) Magnetic Resonance Elastography of Liver: Current Update. Top Magn Reson Imaging 27 (5):319–333. doi:10.1097/RMR.0000000000000177 [PubMed: 30289828]
42. Mathew RP, Venkatesh SK (2018) Imaging of Hepatic Fibrosis. Curr Gastroenterol Rep 20 (10):45. doi:10.1007/s11894-018-0652-7 [PubMed: 30159792]
43. Popov Y, Sverdlov DY, Sharma AK, Bhaskar KR, Li S, Freitag TL, Lee J, Dieterich W, Melino G, Schuppan D (2011) Tissue transglutaminase does not affect fibrotic matrix stability or regression of liver fibrosis in mice. Gastroenterology 140 (5):1642–1652. doi:10.1053/j.gastro.2011.01.040 [PubMed: 21277850]
44. Neef M, Ledermann M, Saegesser H, Schneider V, Reichen J (2006) Low-dose oral rapamycin treatment reduces fibrogenesis, improves liver function, and prolongs survival in rats with

established liver cirrhosis. J Hepatol 45 (6):786–796. doi:10.1016/j.jhep.2006.07.030 [PubMed: 17050028]

45. Erstad DJ, Farrar CT, Ghoshal S, Masia R, Ferreira DS, Chen YI, Choi JK, Wei L, Waghorn PA, Rotile NJ, Tu C, Graham-O'Regan KA, Sojoodi M, Li S, Li Y, Wang G, Corey KE, Or YS, Jiang L, Tanabe KK, Caravan P, Fuchs BC (2018) Molecular magnetic resonance imaging accurately measures the antifibrotic effect of EDP-305, a novel farnesoid X receptor agonist. Hepatol Commun 2 (7):821–835. doi:10.1002/hep4.1193 [PubMed: 30027140]
46. Levine D, McDonald RJ, Kressel HY (2018) Gadolinium Retention After Contrast-Enhanced MRI. JAMA 320 (18):1853–1854. doi:10.1001/jama.2018.13362 [PubMed: 30208489]
47. Le Fur M, Caravan P (2019) The biological fate of gadolinium-based MRI contrast agents: a call to action for bioinorganic chemists. Metallomics 11 (2):240–254. doi:10.1039/c8mt00302e [PubMed: 30516229]
48. Farrar CT, Gale EM, Kennan R, Ramsay I, Masia R, Arora G, Looby K, Wei L, Kalpathy-Cramer J, Bunzel MM, Zhang C, Zhu Y, Akiyama TE, Klimas M, Pinto S, Diyabalanage H, Tanabe KK, Humblet V, Fuchs BC, Caravan P (2018) CM-101: Type I Collagen-targeted MR Imaging Probe for Detection of Liver Fibrosis. Radiology 287 (2):581–589. doi:10.1148/radiol.2017170595 [PubMed: 29156148]
49. Salarian M, Turaga RC, Xue S, Nezafati M, Hekmatyar K, Qiao J, Zhang Y, Tan S, Ibhagui OY, Hai Y, Li J, Mukkavilli R, Sharma M, Mittal P, Min X, Keilholz S, Yu L, Qin G, Farris AB, Liu ZR, Yang JJ (2019) Early detection and staging of chronic liver diseases with a protein MRI contrast agent. Nat Commun 10 (1):4777. doi:10.1038/s41467-019-11984-2 [PubMed: 31664017]
50. Waghorn PA, Jones CM, Rotile NJ, Koerner SK, Ferreira DS, Chen HH, Probst CK, Tager AM, Caravan P (2017) Molecular Magnetic Resonance Imaging of Lung Fibrogenesis with an Oxyamine-Based Probe. Angew Chem Int Ed Engl 56 (33):9825–9828. doi:10.1002/anie.201704773 [PubMed: 28677860]
51. Akam EA, Abston E, Rotile NJ, Slattery HR, Zhou IY, Lanuti M, Caravan P (2020) Improving the reactivity of hydrazine-bearing MRI probes for in vivo imaging of lung fibrogenesis. Chemical Science 11 (1):224–231. doi:10.1039/C9SC04821A [PubMed: 32728411]
52. Chen HH, Waghorn PA, Wei L, Tapias LF, Schu Hle DT, Rotile NJ, Jones CM, Looby RJ, Zhao G, Elliott JM, Probst CK, Mino-Kenudson M, Lauwers GY, Tager AM, Tanabe KK, Lanuti M, Fuchs BC, Caravan P (2017) Molecular imaging of oxidized collagen quantifies pulmonary and hepatic fibrogenesis. JCI Insight 2 (11). doi:10.1172/jci.insight.91506
53. Zhu B, Wei L, Rotile N, Day H, Rietz T, Farrar CT, Lauwers GY, Tanabe KK, Rosen B, Fuchs BC, Caravan P (2017) Combined magnetic resonance elastography and collagen molecular magnetic resonance imaging accurately stage liver fibrosis in a rat model. Hepatology 65 (3):1015–1025. doi:10.1002/hep.28930 [PubMed: 28039886]
54. Atanasova I, Sojoodi M, Leitao HS, Shuvaev S, Geraldes C, Masia R, Guimaraes AS, Tanabe KK, Fuchs BC, Caravan P (2020) Molecular Magnetic Resonance Imaging of Fibrin Deposition in the Liver as an Indicator of Tissue Injury and Inflammation. Invest Radiol 59 (4):209–216. doi:10.1097/RLI.0000000000000631
55. Scotton CJ, Krupiczojc MA, Konigshoff M, Mercer PF, Lee YC, Kaminski N, Morser J, Post JM, Maher TM, Nicholson AG, Moffatt JD, Laurent GJ, Derian CK, Eickelberg O, Chambers RC (2009) Increased local expression of coagulation factor X contributes to the fibrotic response in human and murine lung injury. J Clin Invest 119 (9):2550–2563. doi:10.1172/JCI33288 [PubMed: 19652365]
56. Shea BS, Probst CK, Brazee PL, Rotile NJ, Blasi F, Weinreb PH, Black KE, Sosnovik DE, Van Cott EM, Violette SM, Caravan P, Tager AM (2017) Uncoupling of the profibrotic and hemostatic effects of thrombin in lung fibrosis. JCI Insight 2 (9). doi:10.1172/jci.insight.86608
57. Uppal R, Medarova Z, Farrar CT, Dai G, Moore A, Caravan P (2012) Molecular imaging of fibrin in a breast cancer xenograft mouse model. Invest Radiol 47 (10):553–558. doi:10.1097/RLI.0b013e31825dddfb [PubMed: 22960948]
58. Zhou IY, Jordan VC, Rotile N, Akam EA, Krishnan S, Arora G, Krishnan H, Slattery HR, Warner N, Mercaldo N, Farrar CT, Wellen J, Martinez R, Schlerman F, Tanabe KK, Fuchs BC, Caravan P ((in press)) Advanced MRI of Liver Fibrosis and Treatment Response in a Rat Model of Nonalcoholic Steatohepatitis. Radiology

59. Arena U, Vizzutti F, Corti G, Ambu S, Stasi C, Bresci S, Moscarella S, Boddi V, Petrarca A, Laffi G, Marra F, Pinzani M (2008) Acute viral hepatitis increases liver stiffness values measured by transient elastography. Hepatology 47 (2):380–384. doi:10.1002/hep.22007 [PubMed: 18095306]
60. Petta S, Maida M, Macaluso FS, Di Marco V, Camma C, Cabibi D, Craxi A (2015) The severity of steatosis influences liver stiffness measurement in patients with nonalcoholic fatty liver disease. Hepatology 62 (4):1101–1110. doi:10.1002/hep.27844 [PubMed: 25991038]
61. Eddowes PJ, McDonald N, Davies N, Semple SIK, Kendall TJ, Hodson J, Newsome PN, Flintham RB, Wesolowski R, Blake L, Duarte RV, Kelly CJ, Herlihy AH, Kelly MD, Olliff SP, Hubscher SG, Fallowfield JA, Hirschfield GM (2018) Utility and cost evaluation of multiparametric magnetic resonance imaging for the assessment of non-alcoholic fatty liver disease. Alimentary pharmacology & therapeutics 47 (5):631–644. doi:10.1111/apt.14469 [PubMed: 29271504]
62. Pavlides M, Banerjee R, Tunnicliffe EM, Kelly C, Collier J, Wang LM, Fleming KA, Cobbold JF, Robson MD, Neubauer S, Barnes E (2017) Multiparametric magnetic resonance imaging for the assessment of non-alcoholic fatty liver disease severity. Liver international : official journal of the International Association for the Study of the Liver 37 (7):1065–1073. doi:10.1111/liv.13284 [PubMed: 27778429]
63. Spuentrup E, Ruhl KM, Botnar RM, Wiethoff AJ, Buhl A, Jacques V, Greenfield MT, Krombach GA, Gunther RW, Vangel MG, Caravan P (2009) Molecular magnetic resonance imaging of myocardial perfusion with EP-3600, a collagen-specific contrast agent: initial feasibility study in a swine model. Circulation 119 (13):1768–1775. doi:10.1161/CIRCULATIONAHA.108.826388 [PubMed: 19307474]
64. Caravan P, Yang Y, Zachariah R, Schmitt A, Mino-Kenudson M, Chen HH, Sosnovik DE, Dai G, Fuchs BC, Lanuti M (2013) Molecular magnetic resonance imaging of pulmonary fibrosis in mice. Am J Respir Cell Mol Biol 49 (6):1120–1126. doi:10.1165/rcmb.2013-0039OC [PubMed: 23927643]
65. Polasek M, Yang Y, Schuhle DT, Yaseen MA, Kim YR, Sung YS, Guimaraes AR, Caravan P (2017) Molecular MR imaging of fibrosis in a mouse model of pancreatic cancer. Sci Rep 7 (1):8114. doi:10.1038/s41598-017-08838-6 [PubMed: 28808290]
66. Murphy AP, Greally E, O'Hogain D, Blamire A, Caravan P, Straub V (2019) Noninvasive quantification of fibrosis in skeletal and cardiac muscle in mdx mice using EP3533 enhanced magnetic resonance imaging. Magn Reson Med 81 (4):2728–2735. doi:10.1002/mrm.27578 [PubMed: 30394578]
67. Desogere P, Tapias LF, Rietz TA, Rotile N, Blasi F, Day H, Elliott J, Fuchs BC, Lanuti M, Caravan P (2017) Optimization of a Collagen-Targeted PET Probe for Molecular Imaging of Pulmonary Fibrosis. J Nucl Med 58 (12):1991–1996. doi:10.2967/jnumed.117.193532 [PubMed: 28611243]
68. Desogere P, Tapias LF, Hariri LP, Rotile NJ, Rietz TA, Probst CK, Blasi F, Day H, Mino-Kenudson M, Weinreb P, Violette SM, Fuchs BC, Tager AM, Lanuti M, Caravan P (2017) Type I collagen-targeted PET probe for pulmonary fibrosis detection and staging in preclinical models. Sci Transl Med 9 (384). doi:10.1126/scitranslmed.aaf4696
69. Wahsner J, Desogere P, Abston E, Graham-O'Regan KA, Wang J, Rotile NJ, Schirmer MD, Santos Ferreira DD, Sui J, Fuchs BC, Lanuti M, Caravan P (2019) (68)Ga-NODAGA-Indole: An Allysine-Reactive Positron Emission Tomography Probe for Molecular Imaging of Pulmonary Fibrogenesis. J Am Chem Soc 141 (14):5593–5596. doi:10.1021/jacs.8b12342 [PubMed: 30908032]
70. Montesi SB, Izquierdo-Garcia D, Desogere P, Abston E, Liang LL, Digumarthy S, Seethamraju R, Lanuti M, Caravan P, Catana C (2019) Type I Collagen-targeted Positron Emission Tomography Imaging in Idiopathic Pulmonary Fibrosis: First-in-Human Studies. Am J Respir Crit Care Med 200 (2):258–261. doi:10.1164/rccm.201903-0503LE [PubMed: 31161770]

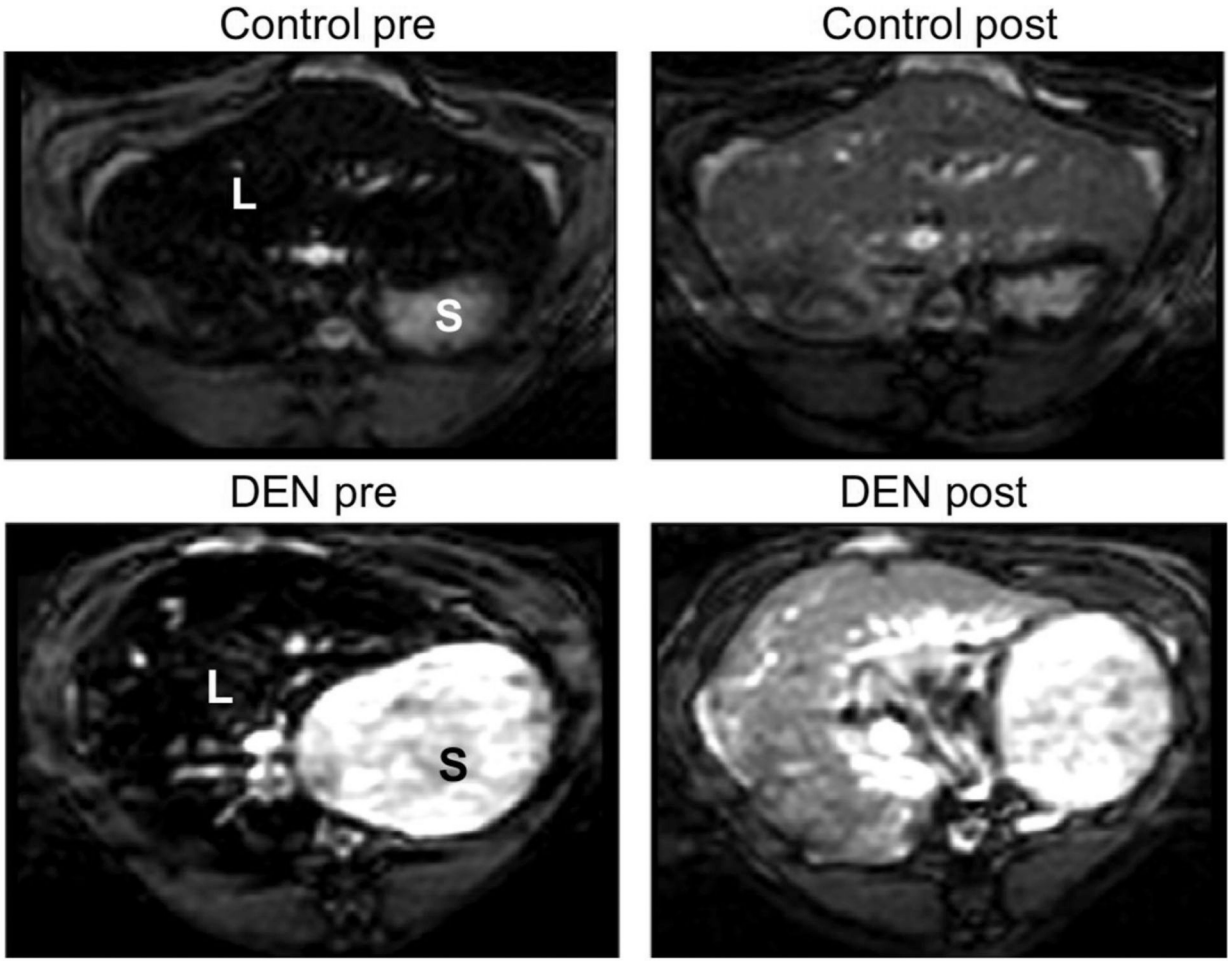

Figure 1.

Molecular MRI of liver fibrosis using the type I collagen-targeted probe EP-3533 in the rat diethylnitrosamine (DEN) model. Inversion recovery MRI of the rat liver before and 40 min after injection of 20 μmol/kg EP-3533; S, stomach; L, liver. The inversion time was chosen to minimize liver signal prior to probe injection. Post-injection, there is a higher signal in the liver of the DEN-treated animal compared to control.

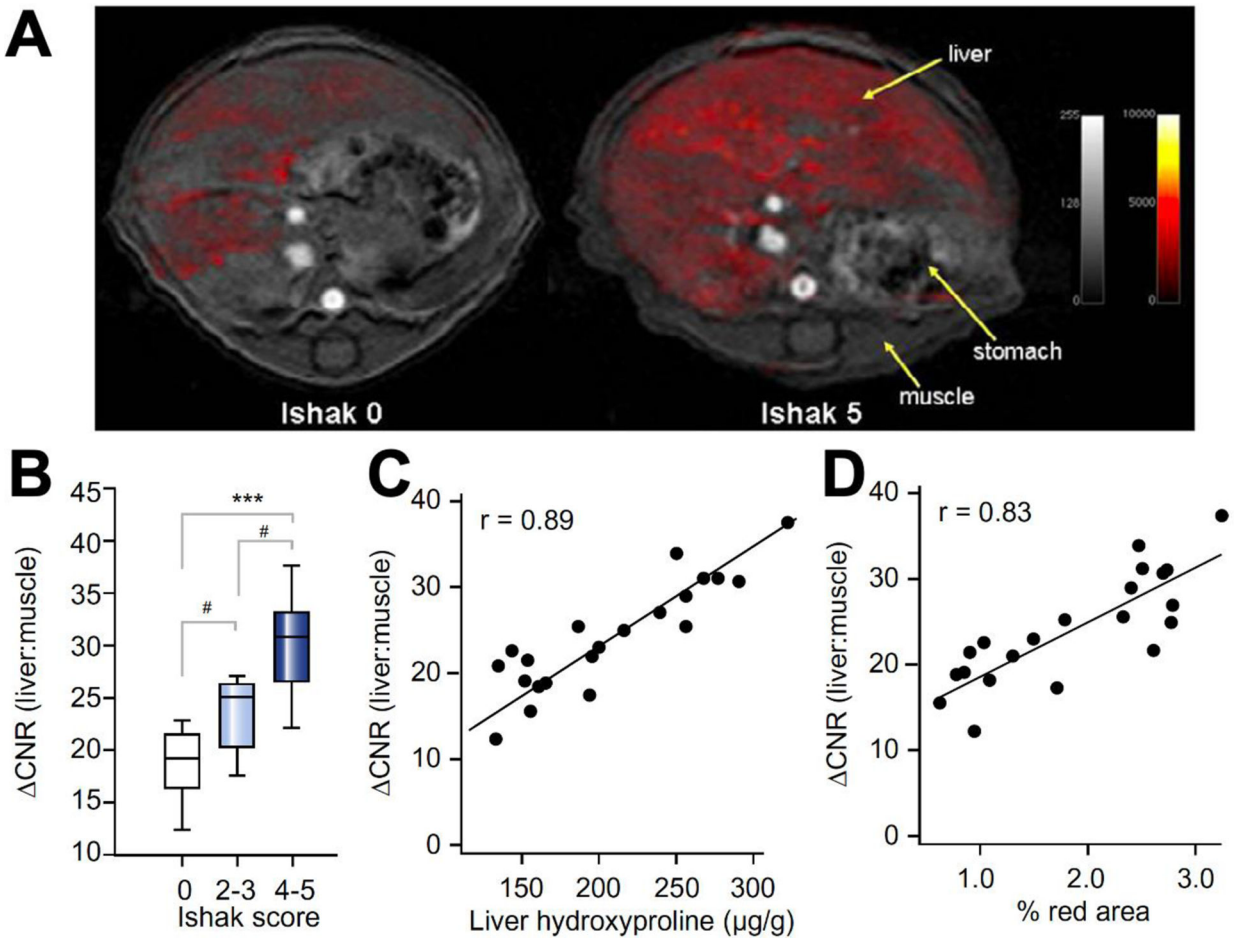

Figure 2.

Staging of liver fibrosis in a mouse CCl_4 model using collagen-enhanced MRI. (A) Representative axial MR images of a control (Ishak 0) and fibrotic (Ishak 5) mouse showing the liver, stomach, and dorsal muscle. False color overlay is the difference image between post- and pre-injection images of EP-3533. Both images rendered at the same scale. (B) ΔCNR (liver:muscle) was calculated as disease progressed as determined by Ishak scoring. (C) Correlation between DCNR (liver:muscle) and total collagen (hydroxyproline). (D) Correlation between DCNR (liver:muscle) and Sirius Red quantification. #p <0.05, *p <0.01 and ***p <0.0001.

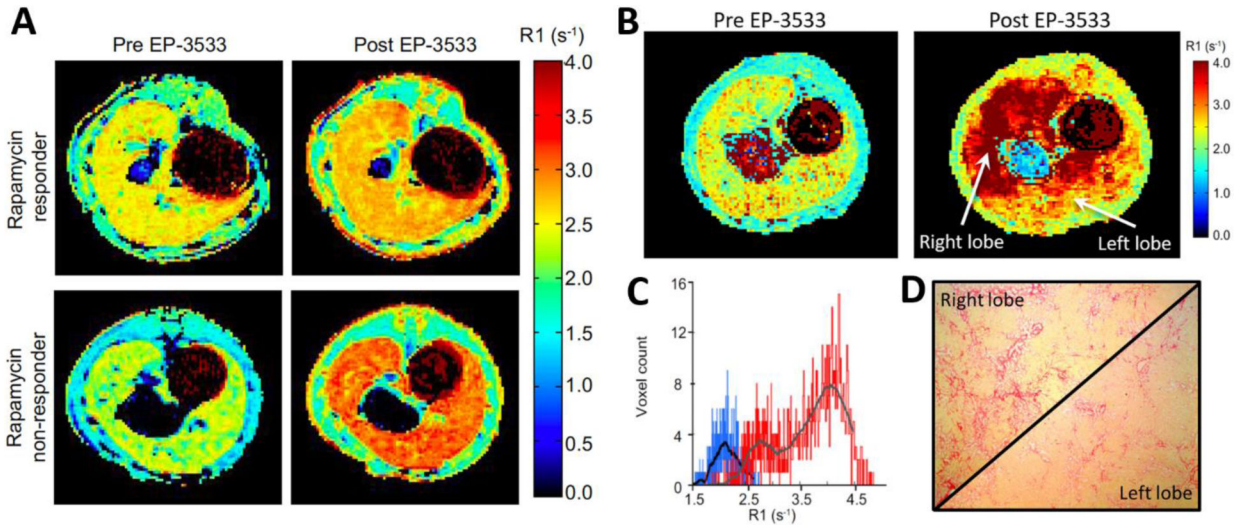

Figure 3.

Collagen imaging captures the variability in treatment response in rapamycin treated bile duct ligated (BDL) rats. (A) Representative longitudinal relaxation rate (R1) maps from a rapamycin responder rat and a rapamycin non-responder acquired pre and post EP-3533. (B) Pre- and post-EP-3533 R1 maps of BDL rat treated with rapamycin. Striking heterogeneity in liver fibrosis with greater R1 in the right liver lobe compared to the left liver lobe. (C) While the pre-EP-3533 histogram (blue) of liver R1 values was homogeneous the post EP-3533 R1 histogram (red) demonstrated a bimodal R1 distribution. (D) Corresponding Sirius Red images from the left and right liver lobes confirmed the fibrosis heterogeneity.

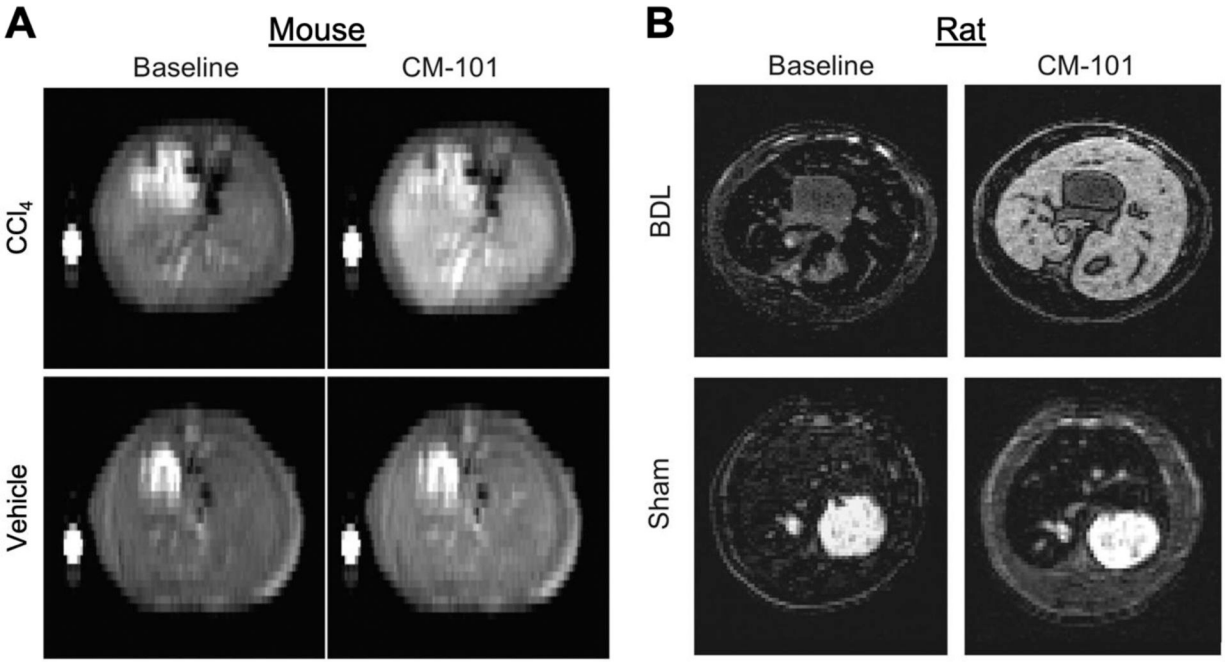

Figure 4.

Type I collagen–targeting macrocycle Gd-DOTA chelate based MRI probe, CM-101, for detection of liver fibrosis in mouse and rat models of liver fibrosis. (A) Representative T1-weighted images acquired pre CM-101 (baseline) and 10 min post CM-101 injection injection for vehicle- and CCl_4-treated mice. (B) Representative T1-weighted images acquired pre CM-101 and 15 min post CM-101 injection in BDL rats and sham-operated rats. Note that the fibrotic liver is markedly enhanced with CM-101 but healthy liver is not.

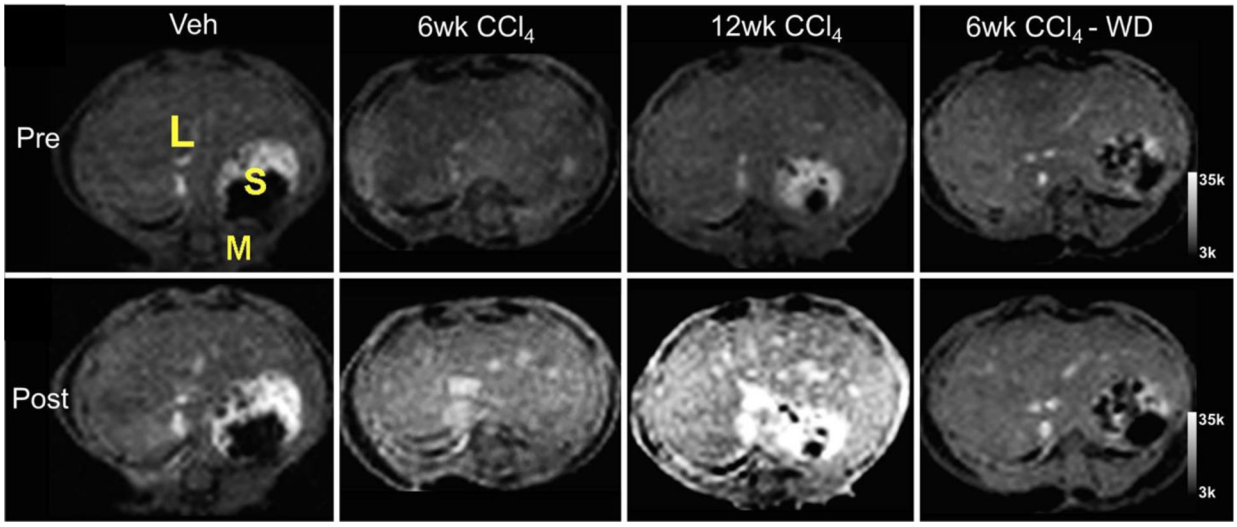

Figure 5.

Fibrogenesis-sensing MRI contrast agent, Gd-Hyd, for detecting hepatic fibrosis progression and regression in CCl_4 mouse model. Representative T1-weighted images before and after Gd-Hyd injection show liver signal enhancement increases with disease severity. In the CCl_4-withdrawal (WD) group, the signal enhancement was not higher than the vehicle-treated controls. L, liver; S, stomach; M, muscle.

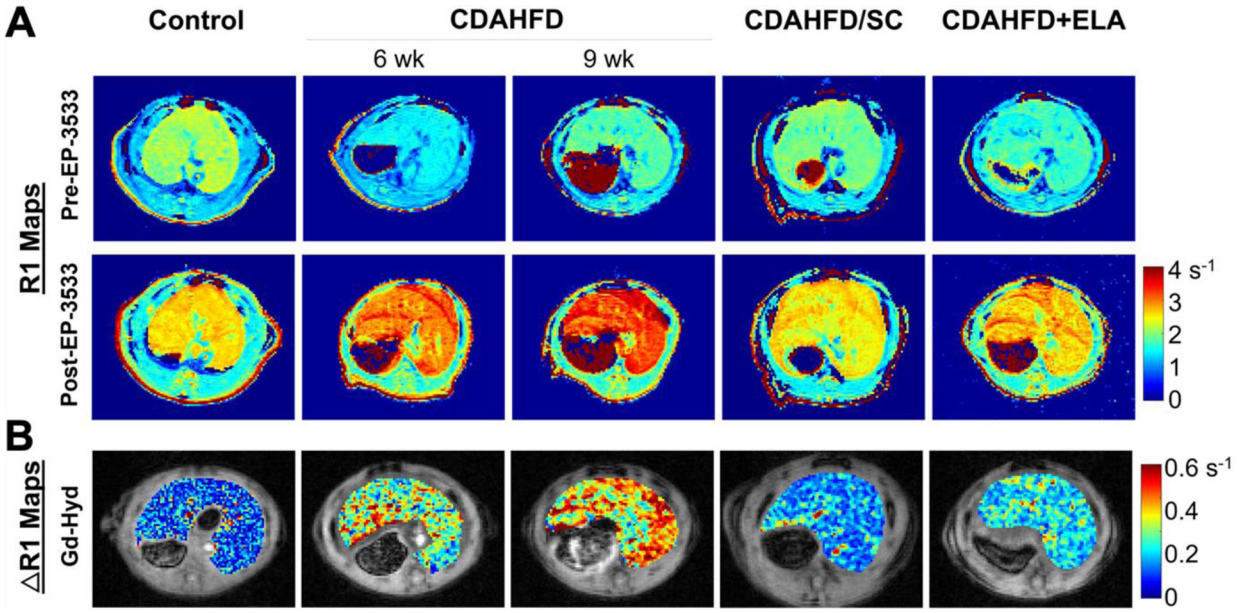

Figure 6.

Multi-parametric MRI with collagen targeted EP-3533 probe in controls, rats fed with choline-deficient, L-amino acid-defined, high-fat diet (CDAHFD) for 6 weeks or 9 weeks, and rats had that received 6 weeks of CDAHFD subsequently either switched back to standard chow for 3 weeks (CDAHFD/SD) or underwent 3 weeks of daily oral gavage of Elafibranor while continuing on CDAHFD (CDAHFD+ELA). (A) Representative axial R1 maps of the liver for each group at baseline and after injection of EP-3533. (B) Representative ΔR1 maps from each group showing the uptake of Gd-Hyd.